Oncogene (2017) **36**, 4445–4456

www.nature.com/onc

ORIGINAL ARTICLE

P53/Rb inhibition induces metastatic adrenocortical carcinomas in a preclinical transgenic model

M Batisse-Lignier[1,2,8], I Sahut-Barnola[1,8], F Tissier[3,4], T Dumontet[1], M Mathieu[1], C Drelon[1], J-C Pointud[1], C Damon-Soubeyrand[1], G Marceau[5], J-L Kemeny[6], J Bertherat[3,7], I Tauveron[1,2], P Val[1], A Martinez[1] and A-M Lefrançois-Martinez[1]

Adrenocortical carcinoma (ACC) is a rare cancer with poor prognosis. Pan-genomic analyses identified p53/Rb and WNT/β-catenin signaling pathways as main contributors to the disease. However, isolated β-catenin constitutive activation failed to induce malignant progression in mouse adrenocortical tumors. Therefore, there still was a need for a relevant animal model to study ACC pathogenesis and to test new therapeutic approaches. Here, we have developed a transgenic mice model with adrenocortical specific expression of SV40 large T-antigen (AdTAg mice), to test the oncogenic potential of p53/Rb inhibition in the adrenal gland. All AdTAg mice develop large adrenal carcinomas that eventually metastasize to the liver and lungs, resulting in decreased overall survival. Consistent with ACC in patients, adrenal tumors in AdTAg mice autonomously produce large amounts of glucocorticoids and spontaneously activate WNT/β-catenin signaling pathway during malignant progression. We show that this activation is associated with downregulation of secreted frizzled related proteins (*Sfrp*) and *Znrf3* that act as inhibitors of the WNT signaling. We also show that mTORC1 pathway activation is an early event during neoplasia expansion and further demonstrate that mTORC1 pathway is activated in ACC patients. Preclinical inhibition of mTORC1 activity induces a marked reduction in tumor size, associated with induction of apoptosis and inhibition of proliferation that results in normalization of corticosterone plasma levels in AdTAg mice. Altogether, these data establish AdTAg mice as the first preclinical model for metastatic ACC.

Oncogene (2017) **36,** 4445–4456; doi:10.1038/onc.2017.54; published online 3 April 2017

INTRODUCTION

Adrenocortical carcinoma (ACC) is a rare tumor with an estimated incidence between 1 and 2 per million per year in adults.[1] However, it is associated with poor prognosis with a 5-year survival rate below 35% in most series.[1,2] Medical treatments such as mitotane and cytotoxic chemotherapy show limited and controversial therapeutic potential, making surgery the only available curative therapy. However, this is associated with low post-operative disease free survival due to high tumor recurrence rate.[3] Better knowledge of the pathophysiology is essential to improve prognosis and to propose more effective therapies.

Large-scale OMICs analyses of ACC have shown that over-expression of IGF2 and constitutive activation of WNT/β-catenin signaling are the two most frequent alterations in ACC patients (reviewed in refs 4 and 5). However, using a number of transgenic mouse models, we and Dr Hammer's group have shown that these two alterations are not sufficient to explain malignant ACC progression, even though constitutive β-catenin activation is sufficient to trigger systematic development of benign adrenal cortex tumors.[6–9]

The third most frequent alteration in ACC patients is characterized by inactivation of the TP53/RB pathway. The tumor suppressor gene *TP53* is located at the 17p13 locus and p53 protein controls a variety of proliferative processes. Germline mutations in *TP53* are identified in 70% of families with Li-Fraumeni syndrome and are associated with susceptibility to ACC.[10] Genetic studies have shown a link between a specific TP53 exon 10 mutation distinct from Li-Fraumeni criteria and 97% of Brazilian pediatric ACC cases.[11,12] Somatic mutations or loss of heterozygosity at the *TP53* locus were found in 25–35% of sporadic ACC in adults[13,14] and overall survival was significantly decreased in ACC patients harboring *TP53* polymorphisms and *RB1* inactivationg mutations.[15,16] Pan-genomic clustering analyses confirmed that p53/Rb and WNT/β-catenin pathways were the most frequently altered pathways in ACC with poorest outcome defined as molecular class C1A[17–19] or CoCII-III.[20]

The simian virus 40 (SV40) large T antigen (TAg) is commonly used as an oncogene acting through its ability to sequester p53 and Rb proteins. Although TAg has already been used to engineer mouse models of adrenal tumors, neoplastic development in these mice was dependent on gonadectomy, which questioned their relevance to human adrenal cortex tumors.[21] In an attempt to propose a more relevant model of adrenal tumorigenesis we have engineered the AdTAg transgenic mouse model in which the *Akr1b7* promoter was used to target TAg expression in the adrenal cortex.[22] Here, we show that 100% of the transgenic progeny from male founder #7 develop bilateral malignant adrenal tumors past the age of 7 months associated with frequent lung and liver

[1]CNRS UMR6293, GReD, INSERM U1103, Université Clermont Auvergne, Aubière, France; [2]Centre Hospitalier Universitaire, Endocrinology Diabetology & Metabolic Diseases Department, School of Medicine, Clermont-Ferrand, France; [3]Department of Pathology, Reference Center for Rare Adrenal Diseases, Assistance Publique Hôpitaux de Paris, Hôpital Cochin, Paris, France; [4]Department of Pathology, Hôpital Pitié-Salpêtrière, Université Pierre & Marie Curie, Paris, France; [5]Centre Hospitalier Universitaire, Department of Biochemistry and Molecular Biology, Clermont-Ferrand, France; [6]Department of Anatomopathology, Clermont-Ferrand Hospital, Clermont-Ferrand, France and [7]Institut Cochin, Université Paris Descartes, INSERM U1016, CNRS UMR8104, Paris, France. Correspondence: Dr A Martinez or Professor A-M Lefrançois-Martinez, GReD, CNRS UMR6293, INSERM U1103, Université Clermont Auvergne, Campus Universitaire des Cézeaux, 10 avenue Blaise Pascal, TSA 60026, 63178 Aubière, France.
E-mail: antoine.martinez@uca.fr or a-marie.lefrancois-martinez@uca.fr
[8]These authors contributed equally to this work.
Received 23 September 2016; revised 20 December 2016; accepted 4 February 2017; published online 3 April 2017

metastases. Sequential analysis of the tumorigenic process in AdTAg mice established that histological, endocrine and molecular characteristics of these tumors are closely matched with human ACC, including spontaneous WNT/β-catenin pathway activation. Moreover, we identified activation of mTOR pathway as an early step in the tumorigenic process and confirmed this activation in a discovery cohort of human adult sporadic adrenocortical tumors. Preclinical targeting of mTOR pathway with Rapamycin resulted in decreased tumor burden and normalization of endocrine activity. Altogether, this suggests that AdTAg mice develop aggressive and metastatic tumors resembling the poor outcome C1A subtype of ACC and can provide a good model for preclinical studies.

RESULTS

Expression of SV40 TAg and tumor formation

In order to develop a transgenic model of adrenocortical carcinoma, we targeted expression of the early region of SV40 large tumor antigen (TAg) to the adrenal cortex of mice, using the *Akr1b7* gene 0.5- kb promoter/intron regulatory sequences as previously described.[22] The resulting mouse transgenic lines were named AdTAg. Female founder #1 showed huge adrenal tumors at the age of 4 months but had to be euthanized before she could be used for breeding. Its right adrenal tumor was used to derive the ATC1 cell line.[22] As illustrated in Figure 1A, 100% of the AdTAg male founder #7 progeny developed huge bilateral adrenal tumors at the age of 8 months resulting in an average increase in adrenal weight ranging from 16- to 300-fold.

AdTAg adrenal histology was compared with WT after hematoxylin/eosin staining and TAg immunohistochemistry on adrenal sections at birth, 2, 4 and 8 months. At birth, consistent with the few scattered cells expressing TAg (Figure 1B(i)), no histological abnormality of the whole gland including cortex was observed (Figure 1B(e)). At 2 months, (Figure 1B(f)) although integrity of the *medulla* was preserved, a large invasive ring of small cells with basophilic nuclei and positive TAg nuclear staining (Figure 1B(j)) was observed between *zonae fasciculata* and *glomerulosa*. This layer evolved as multiple nodular tumor masses within the adrenal cortex from mice aged 4–6 months (Figure 1B(g)). At later stages, all mice presented massive TAg-positive tumor masses (Figure 1B(l)) with invasion of the whole gland resulting in disruption of normal cortical and medullary structures (Figure 1B(h)).

The presence of malignant characteristics was evaluated at different stages by calculating Weiss scores.[23] All 2-month-old animals had a Weiss score $\leqslant 2$. On the opposite, 8-month-old adrenals presented criteria of carcinoma (Weiss $\geqslant 3$) with diffuse architecture, capsular invasion, high mitotic rate, abnormal mitoses, and rare clear cells. Altogether, these observations suggested that targeted expression of TAg in the adrenal cortex induced malignant tumor development.

Identity of tumor cells

Identity of tumor cells was determined in adrenal sections from 2-month-old mice by immunofluorescence for differentiation markers. SF-1 nuclear staining, which marks steroidogenic cells was restricted to cortical cells in WT and AdTAg adrenals, including T-antigen (TAg)-positive tumor cells (Figure 2A(a,b)). At later stages, TAg-positive cells were still positive for SF-1, indicating that their steroidogenic identity was maintained throughout the tumorigenic process (Figure 2A(b) inset). As expected,[24] AKR1B7 staining was detected in *fasciculata* and in TAg-positive cells with lower intensity (Figure 2A(c,d)). 20αHSD[25] and DAB2[26] staining were observed in fetal X-zone (Figure 2A(c,d)) and *glomerulosa* (Figure 2A(e,f)) of both wild-type and AdTAg adrenals but not in TAg-positive cells. These data indicated that the TAg tumor cell population had steroidogenic identity, expanded between *zonae glomerulosa* and *fasciculata* and centripetally invaded the cortex.

TAg-expressing SF-1-positive cells expansion was associated with a 5-fold increase in plasma cortisosterone concentrations in 8-month-old AdTAg mice (17.4 ± 7.6 vs 96 ± 39 ng/ml, $n = 6$, $P < 0.01$ in Mann–Whitney test) although it was within the normal range in 4-month-old AdTAg mice. There was a concomitant decrease in ACTH plasma concentration in 8-month-old AdTAg mice (29.7 ± 10.8 vs 15.8 ± 8.7 ng/l, $n = 6$, $P < 0.05$ in Mann–Whitney test) (Figure 2B). Altogether these results suggested that tumor expansion was responsible for a chronic increase in corticosterone plasma levels in AdTAg mice between 4 and 8 months.

Malignancy of AdTAg adrenal tumors

Time-dependent increase in Weiss scores (Figure 1B) and low survival rate (Figure 3A) suggested that AdTAg tumors progressed to high-grade malignancy past 6 months of age. Cyclin E,[27] Ki67[28] and p53[14] have been described as prognostic factors of aggressiveness in human adrenal carcinoma. RT–qPCR analyses showed a significant increase in *Cyclin E* mRNA levels in AdTAg adrenal tumors compared to WT adrenals from 2 months onwards (Figure 3B). This was confirmed by a large increase in the number of Ki67-positive cells in the expanding tumor area (Figure 3C(d)) that eventually reached a proliferative index of 35–55% by 8 months (Figure 3C(f)). As expected, strong nuclear accumulation of p53 was observed as a result of its sequestration by TAg in AdTAg adrenals (Figure 3C(b)). Analysis of phospho-histone H2AX expression, a marker of DNA double-stranded breaks, revealed scattered staining within the tumor in 8-month-old AdTAg adrenals (Supplementary Figure 1A), reflecting progressive accumulation of DNA damages following p53 inactivation. We recently showed that the histone methyl transferase EZH2 was overexpressed in human ACC as the result of p53/Rb/E2F pathway deregulation, which was associated with tumor progression.[29] Consistent with this observation, AdTAg adrenals from 2 months mice showed strong EZH2/Ki67 co-staining within the expanding tumor area while only few EZH2 positive cells were detected in the vicinity of *zona glomerulosa* in WT (Figure 3D). Overexpression of *Ezh2* mRNA was further confirmed at all stages of tumor progression in AdTAg mice by RT–qPCR (Figure 3E). In contrast to human ACC, malignant progression of mouse adrenal tumors did not correlate with upregulation of *Igf2* mRNA levels. However, it was associated with *Igf1* mRNA increase in 8 months AdTAg mice (Supplementary Figure 1B). *IGF2* is located within the same imprinted locus that H19 non-coding mRNA and cyclin-dependent kinase inhibitor *CDKN1C* genes. In human ACC, upregulation of maternally imprinted *IGF2* is frequently associated with downregulation of paternally imprinted *H19/CDKN1C*.[30] Interestingly, RT–qPCR analyses showed downregulation of both *H19* and *Cdkn1c* transcript levels in 8-month-old but not in younger AdTAg mice (Figure 3E).

A striking feature of adrenal tumors found in 8-month-old but not 4-month-old AdTAg mice was the high frequency (23/35, 66%) of metastatic spread to the lung (21/23, 91%) and the liver (6/23, 26%) or to other sites (5/23, 22%). Hematoxylin/eosin staining and immunohistochemical analyses showed that these nodular masses within the lung or liver parenchyma (Figure 3F) consisted of small cells with basophilic nuclei and TAg-positive nuclear staining (inset in Figures 3F(b) and 3D(e)). To demonstrate the link between primary adrenal tumors and secondary localization, *Sf-1* gene expression was investigated by immunostaining and by RT–qPCR, in liver and lung of WT and transgenic mice. Lung and liver nodules from 8-month-old AdTAg mice showed strong SF-1

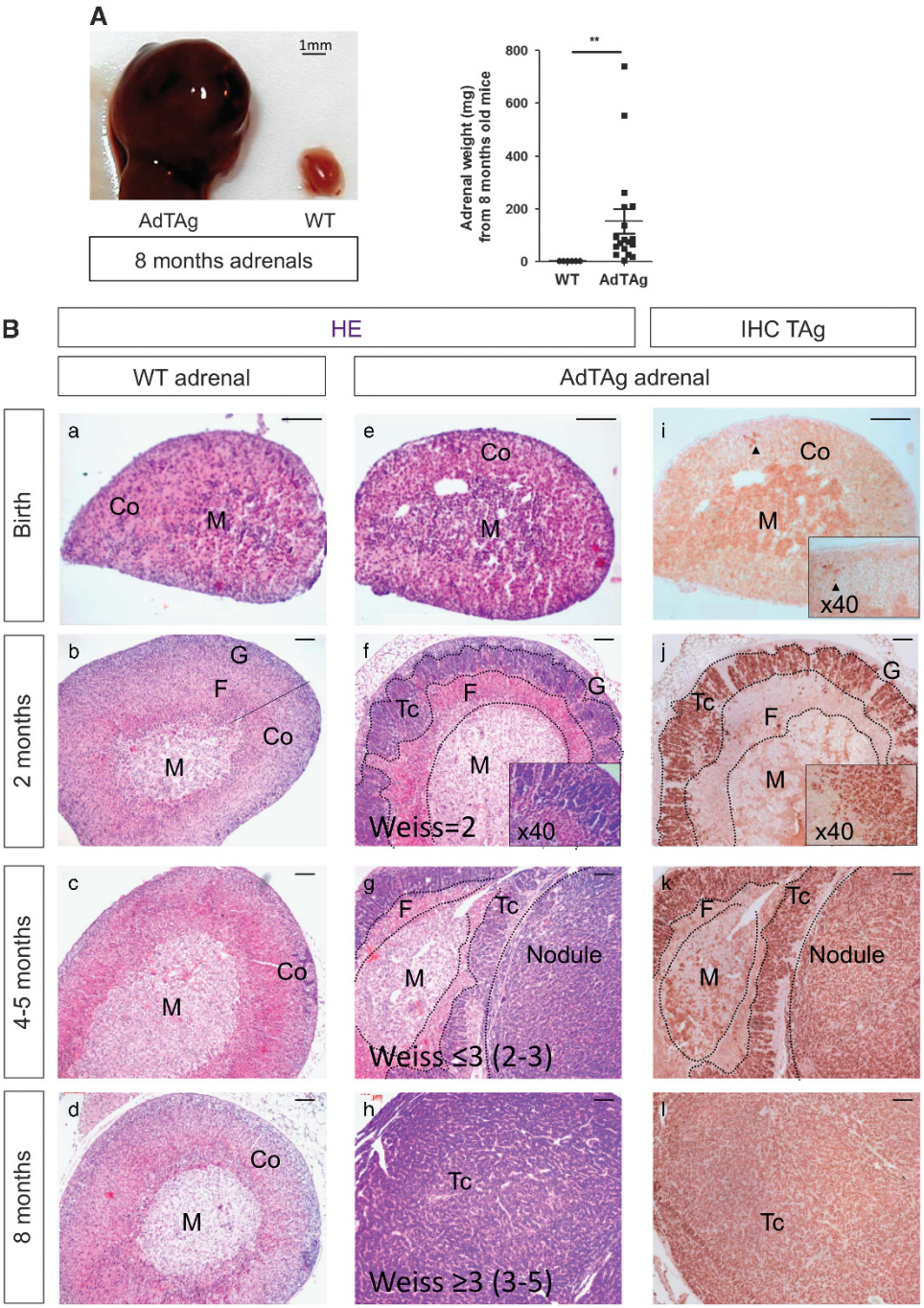

Figure 1. Expression of the Akr1b7:TAg transgene induces adrenal tumors. (**A**) Left: gross adrenal anatomy in 8-month-old AdTAg and WT mice. Right: mean adrenal weights of 8-month-old WT ($n=6$) and AdTAg mice ($n=19$). Adrenals were weighted after dissection of peri-adrenal adipose tissue. Bars represent the mean value of adrenal in WT and AdTAg mice ± s.d. $^{**}P<0.01$, Mann–Whitney test. (**B**) Histological analysis of the adrenal phenotype. Hematoxylin/eosin staining of wild-type adrenal (a–d) and AdTAg adrenals (e–h) at birth ($n=8$), 2 ($n=20$), 4–5 ($n=20$) and 8 months ($n=20$). Weiss score was determined by a trained pathologist, using the criteria defined by Weiss for human adrenal tumors. (i–l) Immunohistochemical analysis of TAg expression in transgenic mice at birth ($n=8$), 2 ($n=10$), 4 ($n=10$) and 8 months ($n=10$). Dotted lines delineate medullary, cortical compartments and tumoral cells that invade the cortex. (g) Zona glomerulosa; (f) zona fasciculata; M, medulla; Co, cortex; Tc, tumoral cells. Scale bar: 100 μm.

staining and high *Sf-1* mRNA accumulation, in contrast with adjacent normal tissue and wild-type corresponding tissues, respectively (Figure 3F(c,f) and Supplementary Figure 2). Altogether these data indicated that advanced adrenal tumors found in AdTAg mice developed lung and/or liver metastases reminiscent of human ACC.

WNT/β-catenin pathway in AdTAg adrenal tumors

Constitutive activation of WNT/β-catenin signaling is found in about 40% of ACC in patients.[31] Although TP53 inactivation was initially described as being mutually exclusive with WNT pathway activation,[32] pan-genomic clustering data showed that about 24% of patients harbor both alterations.[19,20] Importantly, these tumors

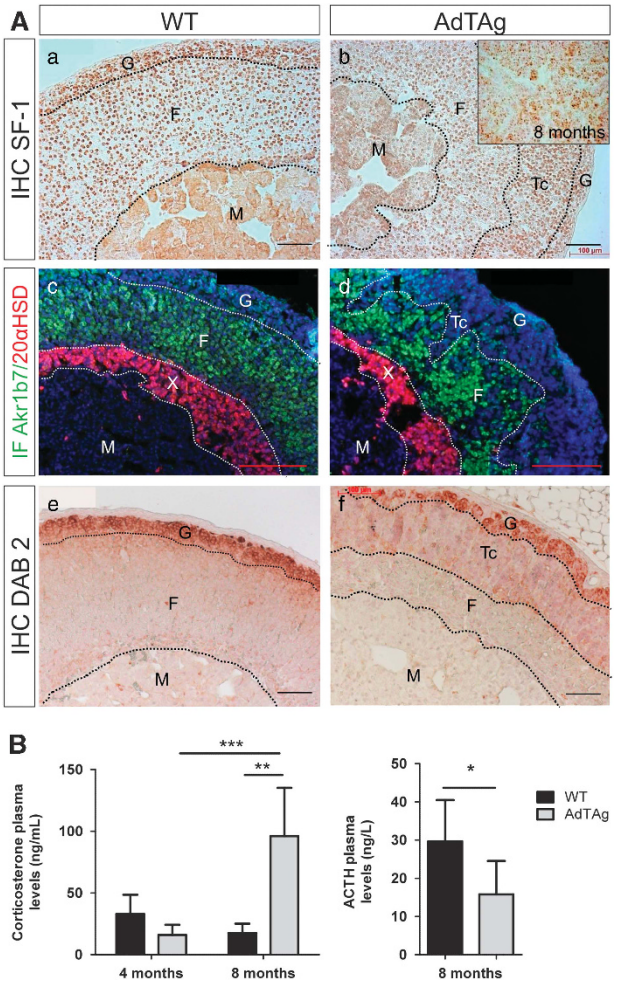

Figure 2. Tumoral cells in AdTAg adrenals have a steroidogenic identity. (**A**) Analysis of SF-1, 20αHSD, AKR1B7 and DAB2 and expression in WT and AdTAg adrenals. (a and b) Immunodetection of SF-1, a steroidogenic marker, in adrenal sections of 2-month-old WT ($n=5$) and 2- and 8-month-old (inset) AdTAg ($n=5$) male mice. (c and d) Adrenal sections from 2-month-old females ($n=5$) double-stained for 20αHSD, a X-zone marker (red) and for AKR1B7, a zona fasciculata marker (green). Nuclei were stained by Hoechst in blue. (e and f) Immunodetection of DAB2, a zona glomerulosa marker, in adrenal sections of 2-month-old WT ($n=5$) and AdTAg ($n=5$) male mice. Dotted lines delineate medullary, cortical compartments and tumoral cells that invade the cortex. G, zona glomerulosa; F, zona fasciculata; M, medulla; X, fetal X-zone; Tc, tumoral cells. Scale bar: 100 μm. (**B**) Left: quantitative analysis of plasma corticosterone in WT mice ($n=6$) compared with AdTAg mice ($n=6$) at 4 and 8 months. Bars represent the mean plasma corticosterone concentration of six individuals in WT and AdTAg mice ± s.d. Right: quantitative analysis of plasma ACTH in WT mice ($n=6$) compared with AdTAg mice ($n=6$) at 8 months. Bars represent the mean ACTH concentration of six individuals in each group. *P*-value was determined by Mann–Whitney test. $^{***}P<0.001$; $^{**}P<0.01$; $^{*}P<0.05$.

mostly belong to the aggressive C1A (CoCII-III) subgroup of poorest survival. In order to assess the role of β-catenin in tumor development, we analyzed co-expression of TAg and β-catenin by immunofluorescence on adrenal sections from 2-, 4- and 8-month-old AdTAg mice. As previously described in wild-type adrenals,[33] β-catenin staining was also restricted to *zona glomerulosa* in 2-month-old AdTAg adrenals (Figure 4A(a,b)). From the age of 4 months, this β-catenin cytoplasmic accumulation extended within tumor areas containing TAg-positive cells (Figure 4A(d)). At this stage, a small number of tumor cells with nucleus and cytoplasmic staining attesting of activation of the pathway were observed (yellow nuclear staining). In animals with more advanced tumor development (8 months), a large number of TAg-positive cells displayed cytoplasmic and/or nuclear accumulation of β-catenin staining (Figure 4A(f)). In good agreement with immunohistological observations, western blot analyses indicated a significant increase in the ratio of activated β-catenin (dephosphorylated) over total β-catenin in adrenal extracts from 8 months AdTAg mice (Figure 4B). This was further confirmed by overexpression of WNT/β-catenin target genes *Axin 2* and *c-Myc* (Figure 4C) in 8-month-old AdTAg adrenals. Although activating mutations of *CTNNB1* were found in 16% ACC patients,[19,31] sequencing of *Ctnnb1* third exon did not reveal any mutation in 8-month-old AdTAg adrenals (not shown). In contrast, a base substitution G to A transition in 3′ splice-acceptor site of intron 2-3 was identified (exon 3 Ivs -1 G->A) in ATC1 cells line that was derived from an advanced TAg-induced adrenal tumor of the founder mice #1.[22] This mutation is predicted to lead to exon 3 skipping as confirmed by cDNA sequencing (Supplementary Figure 3). As expected, western blot analysis (Figure 4B) showed that ATC1 cells expressed a truncated β-catenin comigrating with the previously described transdominant Δex3 β-catenin form expressed in Δcat mice.[33] Recent OMICs analyses have shown that WNT pathway activation in ACC patients without *CTNNB1* mutations was associated with loss of the negative feedback regulator ZNRF3.[19] Interestingly, even though expression of *Znrf3* was not extinguished in AdTAg adrenals, it was significantly decreased in malignant tumors (Figure 5). Concomitantly, *Sfrp1* and *Sfrp5* two members of the secreted frizzled related proteins encoding extracellular inhibitors of WNT signaling,[34,35] were also downregulated in mouse ACC (8 months) while *Wnt4* expression, which is essential for physiological WNT pathway activation in the adrenal,[36] was unaltered throughout malignant progression (Figure 5). Of note, *Sfrp1* and *Sfrp5* mRNA levels were transiently upregulated at early time points (2 months). This could be part of a negative feedback mechanism[37] striving to counteract β-catenin activation at the beginning of the tumorigenic process, which would be outdated between 4 and 8 months, in good agreement with the parallel time-dependent activation of WNT signaling (Figure 4). In contrast, expression of *Sfrp2* was strongly upregulated in mouse malignant tumors. Interestingly, even though it is considered as a WNT pathway inhibitor, SFRP2 was also shown to synergistically augment oncogenic activity of WNT ligands in renal and prostate cancers.[38,39] Altogether these data suggest that, consistent with ACC patients, malignant progression in the AdTAg model correlates with β-catenin activation. Therefore, AdTAg mice represent a good model of patients within the C1A (CoCII-III) subgroup of aggressive and poor outcome ACC, associated with both P53 and WNT pathway alterations.

mTOR pathway activity in AdTAg adrenals and human tumors

Data from the literature suggest that p53 can inhibit mTOR activity.[40,41] Consistent with this idea, evidence for *TP53* mutation as the underlying cause of childhood ACC has been associated with increased activation of the IGF-IR/mTOR signaling pathway in these tumors.[42] Interestingly, western blot analyses showed that activated P-mTOR ser2448 level was increased 1.5-fold in 8 months AdTAg adrenal extracts (Figure 6A). *In situ* analyses of mTORC1 downstream targets by immunohistochemistry showed weak P-S6 staining in scarce cells within *zona fasciculata* in wild-type adrenals (Figure 6B(a)), whereas strong staining was detected in a large number of tumor cells in 2-month-old AdTAg mice (Figure 6B(b)). Moreover, similar results were observed for the phosphorylated Eif4E-binding protein 1 (P-4EBP1) staining (Figure 6B(d)), which was already increased from the age of 1 month (not shown). We concluded that mTOR pathway over-activation was an

early event during the TAg-induced tumorigenic process. This finding suggested that mTOR pathway activation could also be relevant in the context of human adult ACC. Indeed, western blot analysis showed a significant 3-fold increase in mTOR and P-mTOR accumulation in adult ACC compared with adenomas (Figure 6C). Immunohistochemical analyses of adult human adrenal samples revealed a strong accumulation of P-S6 in 6 out of 7 malignant tumors (Figure 6D), whereas it was accumulated at high levels in only 1 out of 6 benign human tumors (Supplementary Figure 4; Supplementary Table). These results indicated that mTOR pathway was activated in both human and mouse malignant adrenal tumors. However global mTOR activation was linked to increased phosphorylation in mouse while it relied on increased mTOR protein levels in patients.

Effect of rapamycin treatment on tumor development

Previous studies have shown the efficacy of drugs targeting mTORC1 activity in inhibiting proliferation of ACC cell lines *in vitro*.[43,44] Therefore, we evaluated the effect of rapamycin-dependent mTORC1 inhibition in AdTAg mice after a 3 weeks short-term or a 3 months long-term treatment (Figure 7A).

Immunohistochemical analyzes showed that short-term rapamycin treatment totally suppressed P-S6 accumulation in tumor cells (Figure 7B(a,b)) validating the efficacy of mTORC1 inhibition. Evaluation of apoptosis showed low numbers of cleaved Caspase 3-positive cells in both WT and vehicle-treated AdTAg adrenals (Figure 7B(c,e)). In contrast there was a marked increase in the number of apoptotic tumor cells in the adrenals of AdTAg mice that received rapamycin treatment (Figure 7B(d)). This was not observed in WT rapamycin-treated mice (Figure 7B(f)), suggesting that the effect of the drug was specific to tumor cells. Increased apoptosis in response to rapamycin treatment was associated with decreased proliferation as shown by RT–qPCR analysis of *Pcna* expression (Figure 7C). We thus concluded that rapamycin specifically induced apoptosis in tumor cells and reduced their proliferation.

Consistent with the effect of short-term treatment, long-term rapamycin injections resulted in decreased adrenal tumor size and reduced malignancy (decreased Weiss score) (Figure 7E). In line with rapamycin impact on tumor expansion, corticosterone plasma levels of rapamycin-treated animals were significantly reduced (Figure 7D). These results suggested that rapamycin treatment reduced the expansion of adrenal lesions and normalized steroidogenic output.

DISCUSSION

Herein, we describe the first mouse model that recapitulates hallmarks of adrenocortical cancer in humans. Indeed, AdTAg mice gradually develop tumors of adrenal cortex steroidogenic cells with increasing aggressiveness according to pathological assessments described for human tumors including metastatic spread.[45] Our data suggest that malignant transition in this model likely occurs between 4 and 8 months and is characterized by (1) decreased survival rate, (2) major tumor mass increase, (3) a Weiss score exceeding the cutoff value of 3, (4) a Ki67 proliferative index over 5%, (5) overexpression of cyclin E and of histone methyl transferase EZH2 and downregulation of paternally imprinted *H19/Cdkn1c* and (6) distant metastases in lung and liver. At 8 months of age all AdTAg mice had functional tumors oversecreting corticosterone in the context of suppressed levels of ACTH. This is consistent with the observation of cortisol excess in 50–80% patients with ACC, which was shown to affect long-term survival.[2,46] Endocrine overactivity of mouse tumors was observed despite a reduction in expression of steroidogenic genes (Supplementary Figure 5). This suggests that just as in patients, endocrine hypersecretion in AdTAg mice relies on the major increase in adrenal mass that compensates for the overall dedifferentiation of tumor cells.[47]

Pan-genomic approaches have highlighted the equal contribution of p53/Rb and β-catenin pathways alterations in ACC.[19,20,48] The AdTAg model gives unique access to the dynamics of malignant progression. Although tumor initiation was triggered by p53/Rb sequestration by TAg, malignant progression in AdTAg mice was preceded by the activation of WNT/β-catenin signaling pathway between 4 and 8 months. β-catenin accumulation and *CTNNB1* exon 3 mutations are associated with poor outcome in human ACC.[32] Other mechanisms of WNT pathway activation in ACC include inactivation of the tumor suppressor *APC* (2%) and loss of the negative feedback regulator *ZNRF3* (21%), which is mutually exclusive with *CTNNB1* mutations. Our data show that WNT pathway activation in the adrenal tumors that develop in AdTAg mice may involve more subtle mechanisms that rely on downregulation of key inhibitors of WNT signaling pathway, including *Znrf3*, but also *Sfrps* that have not been involved in WNT pathway deregulation in human ACC. However, it is important to stress that this results in robust activation of WNT signaling, which is also associated with malignant progression in mouse ACC.

Whereas IGF2 overexpression marks up to 90% of ACC and is a strong diagnostic tool and predictor of shorter disease free survival, AdTAg tumors progress through malignancy despite basal *Igf2* expression. Even though this may be considered as an important discrepancy with the human disease, independent reports demonstrated that overexpression of Igf2 has no oncogenic potential in mouse *in vivo*.[7,8] Interestingly, even though IGF2 was initially considered as a driver of the tumorigenic process in ACC, targeted therapies based on IGF2 receptor (IGF1R) were inefficient for treating ACC in patients.[49] This suggests that IGF2 overexpression in ACC could rather be a passenger hit than a driving force for adrenal tumorigenesis.[9] Finally, while TAg mainly acts through the disruption of p53 and Rb binding, we cannot exclude that other pathways, such as *Igf1* overexpression, could also participate in TAg-mediated tumorigenesis in AdTAg mice[50,51] (Supplementary Figure 1B).

ACC are highly invasive and often fatal cancers. Their treatment is a challenging task with complete surgical resection combined with adjuvant mitotane treatment being the only alternative for localized tumors. Currently available treatments combining mitotane with chemotherapy regimens or IGF1R-based inhibitors targeted therapies offer only limited or no benefit for patients, respectively.[52,53] Therefore, there is a need to develop novel therapies. This requires identification of novel targets and availability of relevant models to evaluate their therapeutic potential. Here, we show that AdTAg mice recapitulate the most frequent alterations found in ACC patients. We further identify mTORC1 pathway activation as a relevant alteration in both mouse and human ACC, which occurs at early stages of tumor development in AdTAg mice. How this is achieved in our model is unclear, although it is likely to be the direct consequence of TAg-mediated inactivation of p53 (and not the result of IGF2 or even IGF1 which occurred after mTOR pathway was already activated (Supplementary Figure 1B)). Indeed, there is ample evidence that the tumor suppressor role of p53 not only relies on cell cycle arrest and apoptosis/senescence but also on general inhibition of IGF1/AKT/mTOR pathway to prevent cell growth and division.[40,41,54] Activated mTORC1 pathway was also observed in 85% (6/7) of human ACC and 50% (3/6) of benign adenomas. In agreement with these result, de Martino *et al.* concluded to the presence of activated mTORC1 pathway in a subset of ACC.[55] These data suggest that counteracting mTORC1 activities may be a therapeutic strategy in ACC. *In vitro* studies had shown that mTORC1 inhibitors inhibited proliferation and cortisol production in human ACC cell lines (H295, SW13).[43,44] In the AdTAg model, rapamycin treatment was shown to reduce expansion of adrenal malignant

lesions and to normalize corticosterone production. ACC tumor reduction was reported in 40% of patients (10 patients) receiving a combination of temsirolimus and cixutumumab (a fully human monoclonal antibody inhibiting IGF1R).[56] A partial response with prolonged survival (11 cycles/months) was reported with sunitinib and sirolimus.[57] Conversely, everolimus showed no therapeutic

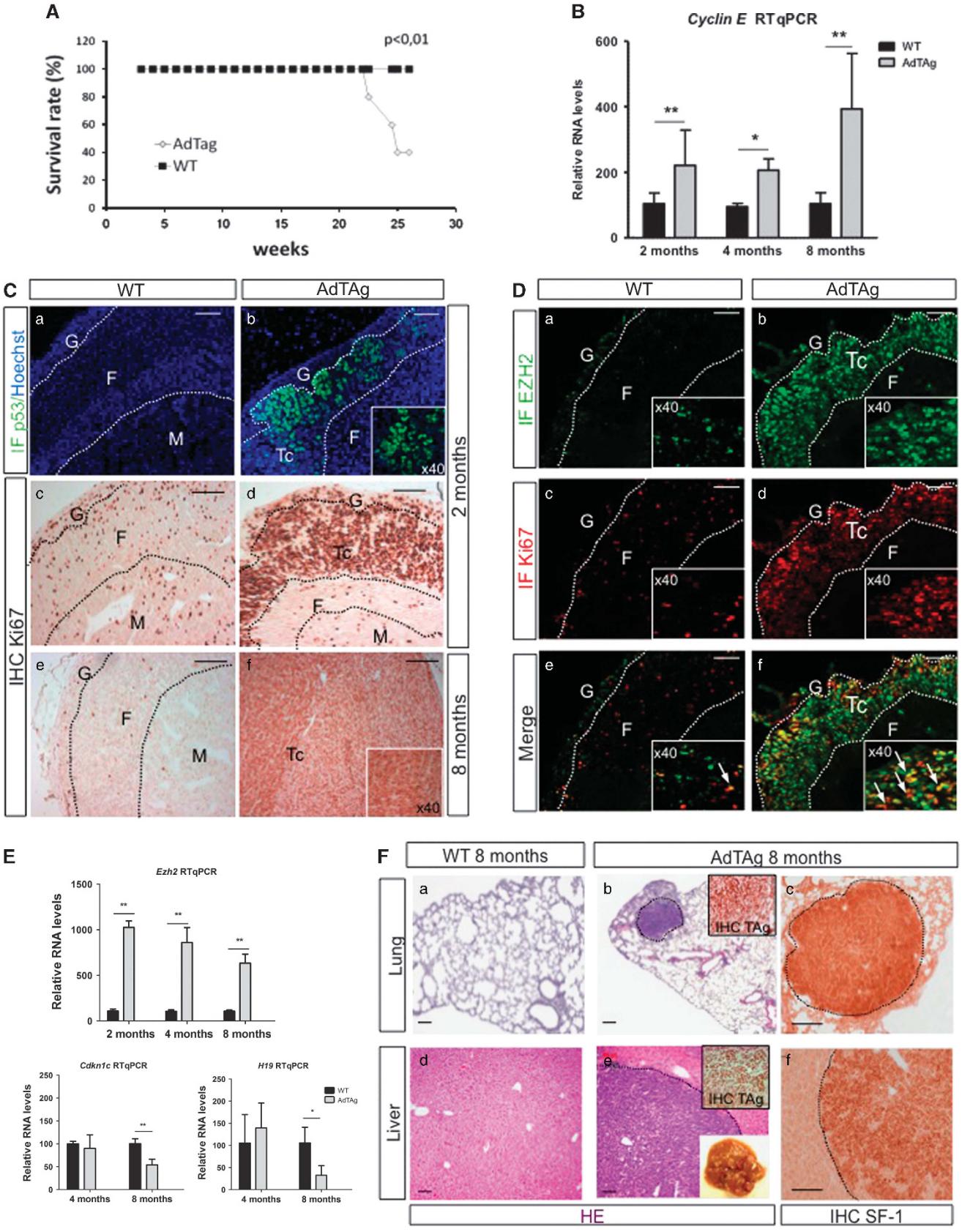

benefit in four patients with progressive metastatic ACC.[58] These contradictory results would suggest that only a subset of ACCs might respond to treatment with mTORC1 inhibitors. In addition, it is possible that activation of other downstream IGF1R effectors may be operative in the pathogenesis of ACC, inducing resistance to mTORC1 inhibitors.

In conclusion, we have developed the first genetically engineered mouse model of adrenal tumorigenesis that recapitulates the

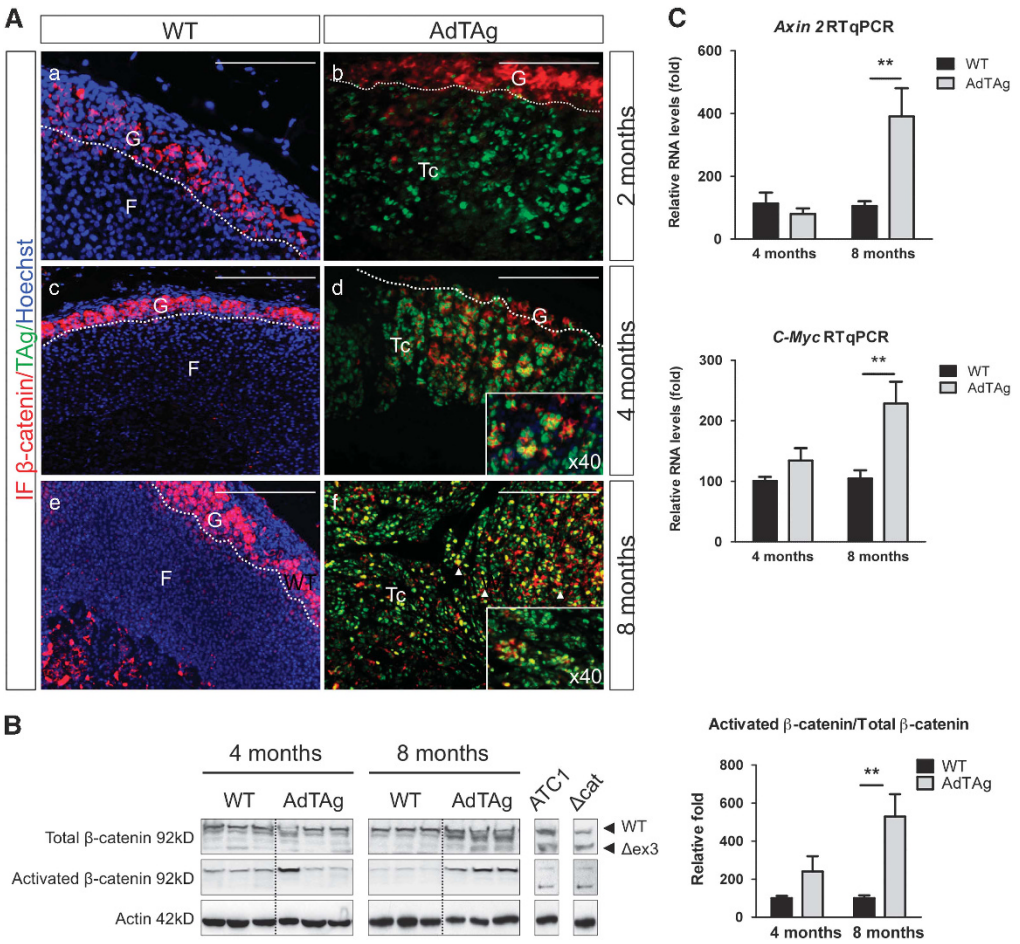

Figure 4. β-catenin signaling pathway is activated in AdTAg adrenals and accompanies carcinoma development. (**A**) Double-stained for β-catenin (red) and for TAg (green) in wild-type ($n=2$) and AdTAg ($n=4$) adrenal sections at 2 (a and b), 4 (c and d) and 8 (e and f) months. Dotted lines delineate cortical compartments and tumoral cells that invade the cortex. (g) Zona glomerulosa; F, zona fasciculata; Tc, tumoral cells. Scale bar: 100 μm. (**B**) Left: Representative Total β-catenin/Activated β-catenin western blotting in 4 and 8 months WT and AdTAg adrenals, ATC1 mouse adrenal carcinoma cells, and Δcat mouse adrenal (transgenic mice with deletion of exon 3 of β-catenin inducing constitutive activation of β-catenin). Right: quantification Activated β-catenin/Total β-Catenin in 4 and 8 months WT and AdTAg adrenals. Bars represent the mean relative quantification of protein expression in 5 adrenals per genotype ± s.d. *P*-value was calculated using Mann–Whitney test. $^{**}P < 0.01$. (**c**) Quantitative representation of mRNA expression of genes encoding Axin 2 and c-Myc in wild-type ($n=6$) and AdTAg ($n=7$) adrenals at 4 and 8 months. Bars represent the mean relative quantification of gene expression in at least 6 adrenals per genotype ± s.d. *P*-value was calculated using Mann–Whitney test. $^{*}P < 0.05$; $^{**}P < 0.01$.

Figure 3. Expression of the Akr1b7:TAg transgene induces adrenal carcinoma in 8-month-old mice. (**A**) Survival curve of WT and AdTAg mice. *P*-value was calculated using Gehan-Breslow-Wilcoxon test. (**B**) Cyclin E expression was analyzed by RT–qPCR with mRNA from wild-type ($n=5$), and AdTAg ($n=5$) adrenals at 2, 4 and 8 months. Bars represent the mean relative quantification of gene expression in 5 adrenals per genotype ± s.d. *P*-value was calculated using Mann–Whitney test. $^{*}P < 0.05$; $^{**}P < 0.01$. (**C**) (a and b) Immunofluorescence detection of p53 in 2-month-old WT ($n=3$) and AdTAg ($n=3$) adrenals. (c–f) Immunostaining for Ki67 in adrenal sections of 2- and 8-month-old WT ($n=3$) and AdTAg mice ($n=4$). (**D**) (a and b) Immunofluorescence detection of EZH2 in 2-month-old WT ($n=3$) and AdTAg ($n=3$) adrenals. (c and d) Immunofluorescence detection of Ki67 in 2-month-old WT ($n=3$) and AdTAg ($n=3$) adrenal. (e and f) Co-immunofluorescence of EZH2 and Ki67 in 2-month-old WT ($n=3$) and AdTAg ($n=3$) adrenals. Dotted lines delineate medullary, cortical compartments and tumoral cells that invade the cortex. (g) Zona glomerulosa; F, zona fasciculata; M, medulla; Tc, tumoral cells. Scale bar: 100 μm. (**E**) *Ezh2*, *H19* and *Cdkn1c* expression levels were analyzed by RT–qPCR with mRNA from wild-type ($n=5$), and AdTAg ($n=5$) adrenals at 2, 4 and 8 months. Bars represent the mean relative quantification of gene expression in 5 adrenals per genotype ± s.d. *P*-value was calculated using Mann–Whitney test. $^{*}P < 0.05$; $^{**}P < 0.01$. (**F**) Eight-month-old mice develop lung and liver metastases. Hematoxylin/eosin staining of WT and transgenic lung (a and b) and liver (d and e). Immunohistochemical detection of TAg in lung and liver metastases of transgenic mice (top insets). Macroscopic view of a metastatic liver is shown (bottom inset). Immunohistochemical detection of SF-1 in lung (c) and liver (f) metastases. Dotted line in b, c and e, f highlights the separation between normal and metastatic tissue in lung and liver. Scale bar: 100 μm.

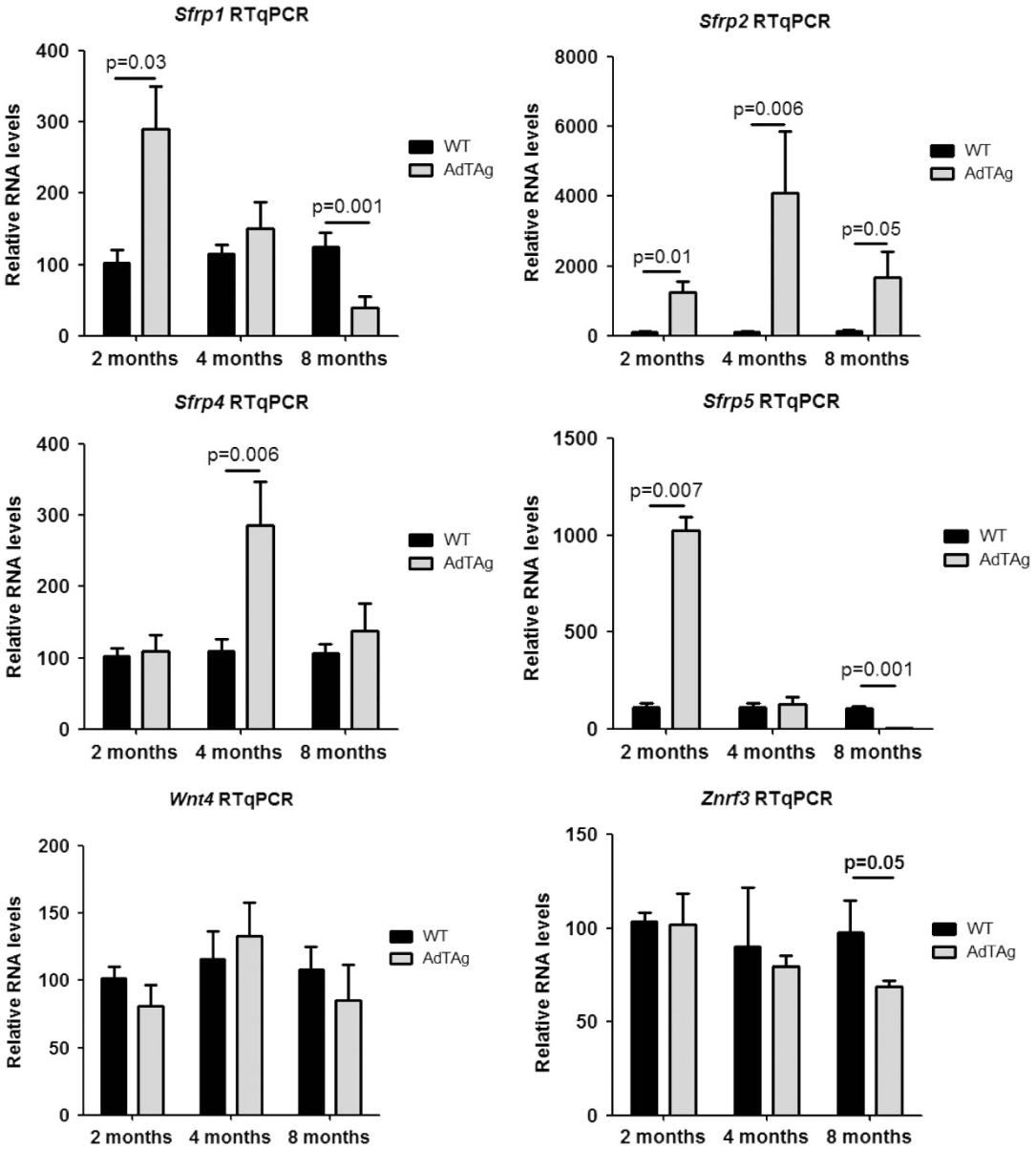

Figure 5. Wnt antagonists expression is differentially regulated in AdTAg adrenal tumors. *Sfrp1-5, Wnt4 and Znrf3* expression was analyzed by RT–qPCR with mRNA from WT ($n = 6$) and AdTAg ($n = 7$) adrenals at 2, 4 and 8 months. Bars represent the mean relative quantification of gene expression in at least 6 adrenals per treatment ± s.d. *P*-value was calculated using Mann–Whitney test. $^*P < 0.05$; $^{**}P < 0.01$.

progression of functional tumors from benign to malignant stages including metastatic invasion. The aggressiveness and the clear evidence that both p53/Rb and WNT/β-catenin pathways are altered during malignant progression make AdTAg mice an animal model for the more aggressive class of ACC related to the the C1A (or CoCII-III) molecular subgroup of tumors with poorest outcome.[17–20] Synchronous and reproducible progression of these tumors over generations, allows framing of important phases of the tumorigenic program such as tumor initiation and malignant transition coinciding with induction of mTOR and β-catenin signaling pathways, respectively. We also provide the proof of concept for using the AdTAg model for preclinical studies with druggable targets.

MATERIALS AND METHODS

Mice

All animal studies were approved by Animal Care Committee (C2E2A Auvergne; protocol CE114-12, CE 113-12) and were conducted in agreement with international standards for animal welfare in order to minimize animal suffering. Transgenic animals were previously described.[22] Genotyping was performed by genomic PCR with primers 5′-GGAATCTTTGCAGCTAATGGA-3′ and 5′-CATCCCAGAAGCTCCAA-3′.

Mice were culled by decapitation at the end of experiments. Blood was collected on vacuum blood collection tube (Terumo) and tissues were immediately fixed in 4% paraformaldehyde or stored at − 80 °C. Littermate control animals were used in all experiments.

Rapamycin treatment

Two and 3.5 months mice were treated five days per week with intraperitoneal injection of rapamycin ($n = 12$) (5 mg/kg/bodyweight/day) or corresponding vehicle ($n = 12$) during 3 weeks or 3 months, respectively. Rapamycin (#R-5000, LC Laboratories) was diluted at a final concentration of 50 µg/mL in a vehicle solution of PBS/10%, tween80/5%, ethanol/5%, cremophor (#C5135, Sigma-Aldrich, St Quentin Fallavier, France).

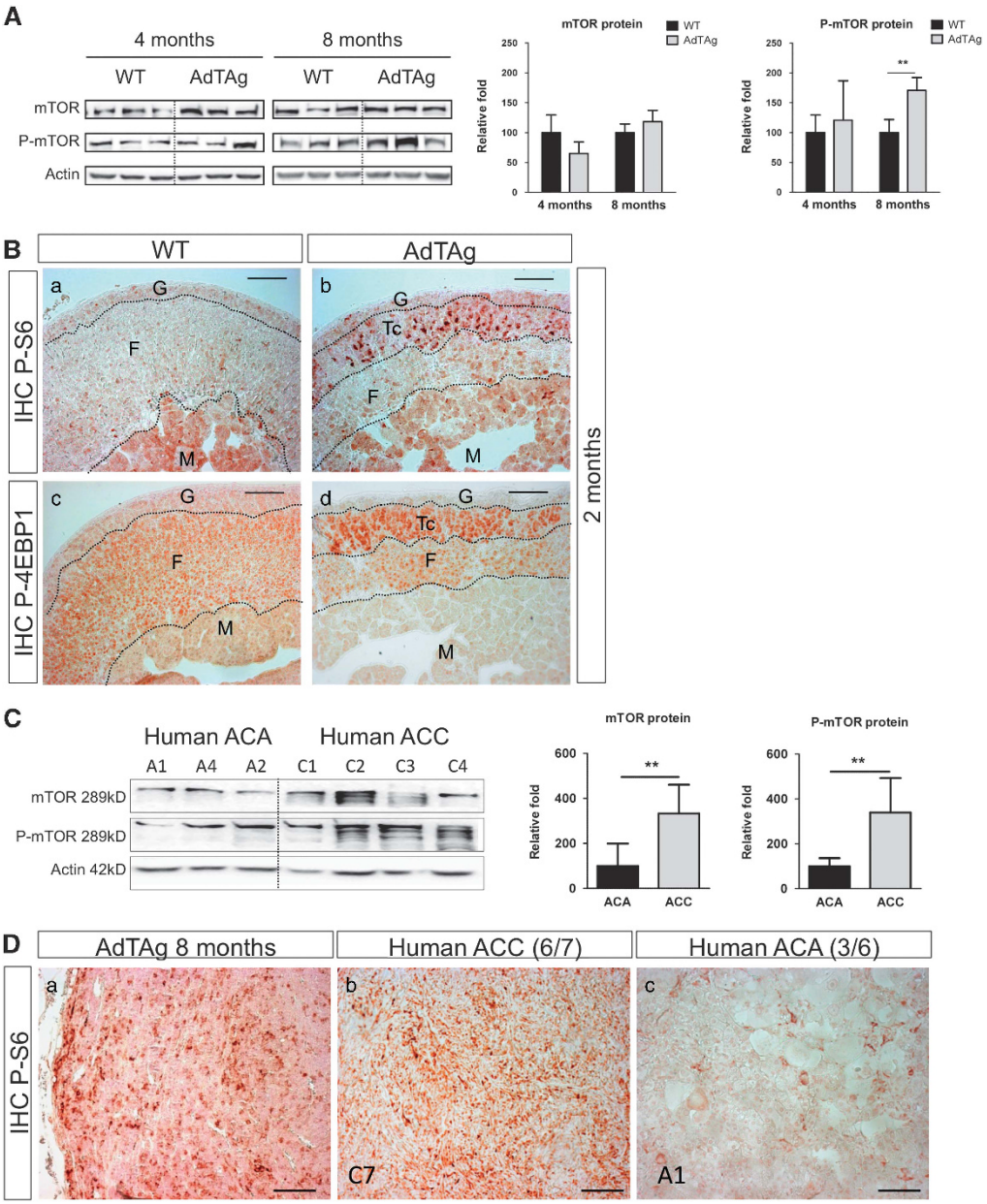

Figure 6. mTOR pathway is activated in AdTAg adrenals and in human adrenal carcinomas. (**A**) Left: representative mTOR, P-mTOR western blotting in 4 and 8 months WT and AdTAg adrenals. Right: quantification mTOR/actin, P-mTOR/actin in 4 and 8 months WT and AdTAg adrenals. Bars represent the mean relative quantification of protein expression in 5 adrenals per genotype ± s.d. *P*-value was calculated using Mann–Whitney test. $^{**}P < 0.01$. (**B**) Immunohistochemical analysis of P-S6 and P-4EBP1 expression in WT ($n = 4$) and AdTAg ($n = 4$) adrenals at 2 months. Dotted lines delineate medullary, cortical compartments and tumoral cells that invade the cortex. G, *zona glomerulosa*; F, *zona fasciculata*; M, *medulla*; Tc, tumoral cells. Scale bar: 100 μm. (**C**) Left: Representative mTOR, P-mTOR western blotting in human ACA and human ACC. Right: quantification mTOR/actin, P-mTOR/actin in human ACA (adrenocortical adenoma) and ACC (adrenocortical carcinoma). Bars represent the mean relative quantification of protein expression in 4 adrenals per group ± s.d. *P*-value was calculated using Mann–Whitney test. $^{**}P < 0.01$. (**D**) Immunohistochemical analysis of P-S6 expression in 8-month-old AdTAg adrenal ($n = 3$) (a), in human adrenocortical carcinoma (ACC) exemplified here by C7 patient (b) and in human adrenocortical adenoma (ACA) illustrated here by A1 patient (c). Scale bar: 100 μm.

Human adrenal tissue

Informed signed consent for the analysis of adrenal tissue was obtained from the patients and the study was approved by an institutional review board (Comité Consultatif de Protection des Personnes dans la Recherche Biomédicale, Cochin Hospital, Paris). Adrenal adenoma and carcinoma paraffin sections were performed for immunohistochemistry analyses.

Immunohistology and western blots

Adrenal were fixed in 4% paraformaldehyde overnight. After two washes in PBS, adrenals were dehydrated through an ethanol gradient and incubated for 2 h in Histoclear (HS200; National Diagnostics, Fisher Scientific, Illkirch, France) and then were embedded in paraffin.

Haematoxylin/eosin staining was performed on 5μM sections with a Microm HMS70 automated processor (Microm Microtech, Francheville, France), according to standard procedures. Primary antibodies (Supplementary Material) were detected with appropriate secondary antibodies, coupled to biotin (1/500, Jackson Immunoresearch, Newmarket, UK). Biotin was then complexed with streptavidin coupled to Horse Radish Peroxidase (HRP) (016-030-084, Jackson Immunoresearch). HRP activity was detected with chromogenic substrate Novared (SK4800, Vector Labs, Peterborough, UK). P53 and

H2AX antibodies were detected by immunofluorescence with secondary antibodies coupled to Alexa488 or Alexa555 (Molecular Probes, Life Technologies, Villebon, France).

Double-immunohistochemistry experiments were performed following a similar protocol. When the two antibodies were raised in different species, the two primary antibodies were sequentially detected by amplification

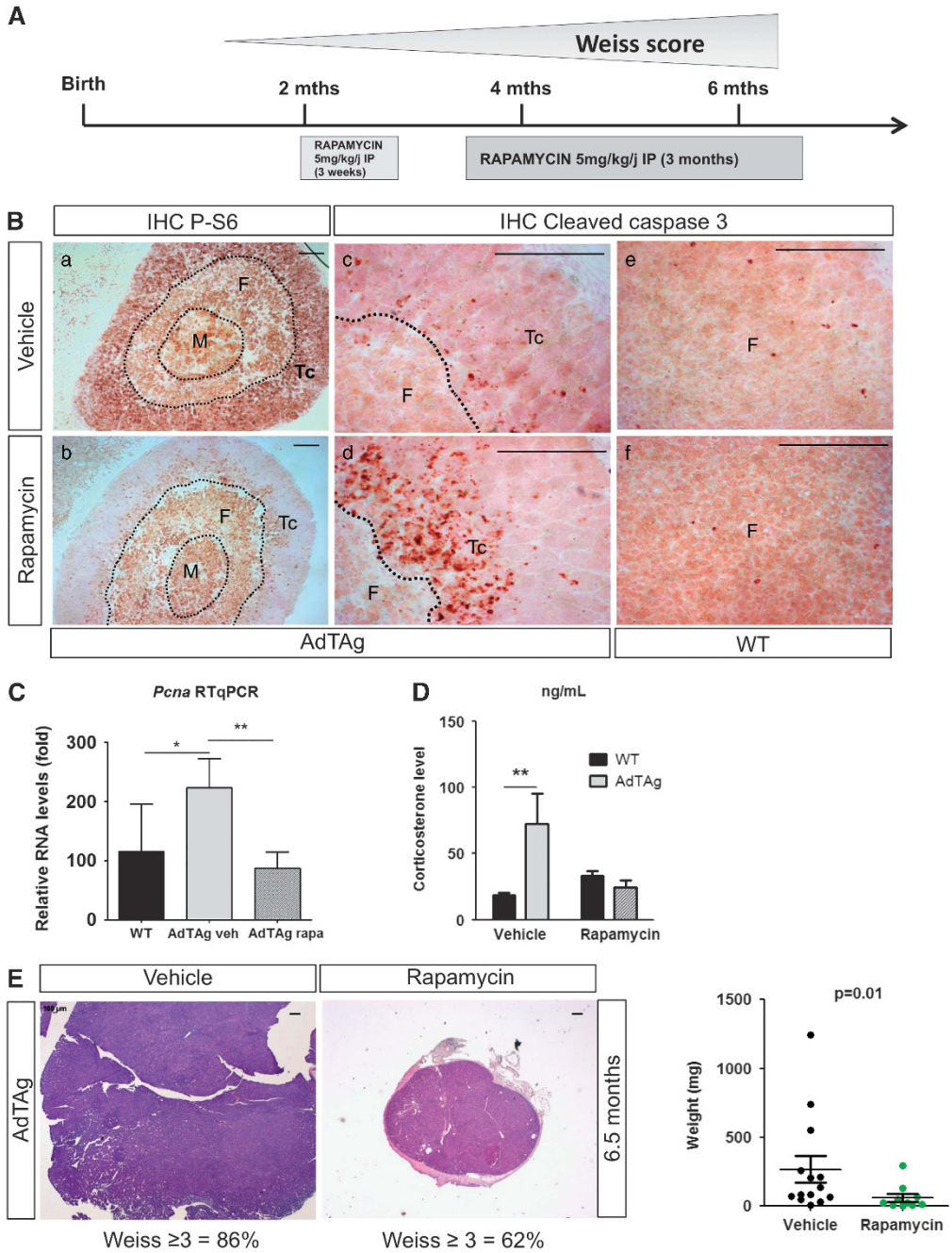

Figure 7. Rapamycin treatment inactivates mTORC1 pathway and inhibits tumor growth. (**A**) Experimental setup of rapamycin treatment in WT and AdTAg mice. Rapamycin (5 mg/kg/day) or corresponding vehicle was given by intraperitoneal injection during 3 weeks (short treatment) or 3 months (long treatment) five days per week. Short treatment was started at the age of 2 months. Long treatment was started at the age of 3.5 months. (**B**) P-S6 (a and b) and cleaved caspase 3 (c–f) expressions were analyzed by immunohistochemistry in 3-month-old WT ($n=6$) and AdTAg ($n=6$) adrenals treated by vehicle or rapamycin during 3 weeks. Dotted lines delineate medullary, cortical compartments and tumoral cells that invade the cortex. F, *zona fasciculata*; M, *medulla*; Tc, tumoral cells. Scale bar: 100 μm. (**C**) *Pcna* expression was analyzed by RT–qPCR with mRNA from 3-month-old wild-type, and AdTAg adrenals treated by vehicle or rapamycin during 3 weeks. Bars represent the mean relative quantification of gene expression in adrenal ($n=6$) per treatment ± s.d. *P*-value was calculated using Mann–Whitney test. $^{*}P<0.05$; $^{**}P<0.01$. (**D**) Quantitative analysis of plasma corticosterone in WT mice ($n=7$) compared to AdTAg mice ($n=5$) at 6.5 months treated by vehicle or rapamycin during 3 months. Bars represent the mean corticosterone concentration in WT (black bar) and AdTAg (gray bar) mice ± s.d. (**E**) Left: Hematoxylin/eosin staining of 6.5-month-old AdTAg adrenal treated by vehicle (a) or rapamycin (b) during 3 months. Scale bar: 200 μm. Right: Mean adrenal weights of 6.5-month-old AdTAg mice treated by vehicle ($n=7$) or rapamycin ($n=5$). Each individual adrenal value was plotted on the graph. Adrenals were weighted after dissection of peri-adrenal adipose tissue. *P*-value was calculated using Mann–Whitney test. Weiss score was determined by a trained pathologist, using the criteria defined by Weiss for human adrenal tumors.

with TSA-Alexa488 and TSA-Alexa555 (Molecular Probes, Life Technologies) fluorescent HRP substrates. To avoid cross-reaction, HRP was inactivated by incubation with 0.02% HCl for 20 min after detection of the first antibody. When the two primary antibodies were raised in the same species, one primary antibody was sufficiently diluted to prevent direct immunodetection and was detected by amplification with TSA-Alexa488 or TSA-Alexa555. The other antibody was subsequently detected by Immunofluorescence with secondary antibodies coupled to Alexa488 or Alexa555.

Microscope image acquisition

Images were acquired at room temperature with a Carl Zeiss Axiocam digital camera on a Zeiss Axioplan 2 microscope. Objectives used were Zeis $\times 10$ (0.30), $\times 20$ (0.50), $\times 40$ (0.75). Image acquisition was performed with Zeiss Axiovision.

Reverse-transcription quantitative PCR

Frozen adrenals were disrupted in Nucleospin RNA II lysis buffer (Macherey Nagel, Hoerdt, France) using the Tissue-Lyser system (Qiagen, Courtaboeuf, France). Total mRNAs were extracted using the NucleoSpin RNA II kit (Qiagen) according to manufacturer's instructions. Five hundred ng of mRNAs were reverse transcribed for 1 h at 42 °C with 5 pmol of random hexamer primers (U1240; Promega), 200 units reverse transcriptase (M1701; Promega), 2 mM dNTPs and 20 units RNAsin (N2615; Promega). A half microliter of one-tenth dilution of cDNA was used in each quantitative PCR reaction. Gene expression levels were measured by RT–qPCR using either probes from the Taqman gene expression assays pool (Applied Biosystem, Life Technologies, Villebon, France) or SYBR green PRC primers. For Taqman analysis, each reaction were performed in duplicated in a final volume of 15 µl with 0.75 µl of the appropriate probe mix and 7.5 µl of PCR Mastermix (Precision, lc., Primerdesign.bo.uk). For SYBR Green analyses, each reaction was performed in duplicate in a final volume of 25 µl with 12.5 µl of MESA Green qPCR mix (Eurogentec) and 10 pmol of forward and reverse primers (Supplementary Material). Relative mRNA accumulation was determined by ΔΔCt method with peptidylprolyl isomerase B (*Ppib*) as standard for Taqman analyses and with *36b4* and *Actin* as standard for SYBR Green analyses. Statistical analyses were performed with Mann–Whitney test.

Hormone measurements

Plasma corticosterone levels were quantified by radio-immunoassay (RIA) using the RIA Corticosterone (3)H kit (MP Biomedicals) according to manufacturer's instructions. ACTH levels in plasma were measured by solid-phase, two-site sequentiel chemiluminescent immunometric assay (Siemens Healthcare Diagnostic SAS, SaintDenis, France) using an Immulite 2000 analyzer.

Statistical analysis

Experimental groups were drawn by lots among animals of the same generation, age and genotype. All data are presented as mean ± s.d. Statistical significance for differences in lesion areas were evaluated using Student's *t*-test or Mann–Whitney test. Differences were considered significant at $P < 0.05$.

CONFLICT OF INTEREST

The authors declare no conflict of interest.

ACKNOWLEDGEMENTS

We thank Lucile Mounier for technical assistance and Sandrine Plantade, Khirredine Ouchen and Philippe Mazuel for animal care. Tissue analyses were performed at Anipath Clermont core facility. This work was supported by Université Blaise Pascal, Université d'Auvergne, CNRS, INSERM, Agence National de la Recherche (grant ANR-14-CE12-0007), grants from Fondation ARC pour la Recherche sur le Cancer (PJA 20141201894) and from La Fondation de France. We thank the Cochin tumor bank and COMETE (COrtico MEdullo Tumeurs Endocrines) network for the provision of ACA and ACC tissue samples.

REFERENCES

1 Allolio B, Fassnacht M. Clinical review: adrenocortical carcinoma: clinical update. *J Clin Endocrinol Metab* 2006; **91**: 2027–2037.
2 Abiven G, Coste J, Groussin L, Anract P, Tissier F, Legmann P *et al.* Clinical and biological features in the prognosis of adrenocortical cancer: poor outcome of cortisol-secreting tumors in a series of 202 consecutive patients. *J Clin Endocrinol Metab* 2006; **91**: 2650–2655.
3 Baudin E. Adrenocortical carcinoma. *Endocrinol Metab Clin North Am* 2015; **44**: 411–434.
4 Else T, Kim AC, Sabolch A, Raymond VM, Kandathil A, Caoili EM *et al.* Adrenocortical carcinoma. *Endocr Rev* 2014; **35**: 282–326.
5 Faillot S, Assie G. ENDOCRINE TUMOURS: The genomics of adrenocortical tumors. *Eur J Endocrinol Eur Fed Endocr Soc* 2016; **174**: R249–R265.
6 Berthon A, Sahut-Barnola I, Lambert-Langlais S, de Joussineau C, Damon-Soubeyrand C, Louiset E *et al.* Constitutive beta-catenin activation induces adrenal hyperplasia and promotes adrenal cancer development. *Hum Mol Genet* 2010; **19**: 1561–1576.
7 Heaton JH, Wood MA, Kim AC, Lima LO, Barlaskar FM, Almeida MQ *et al.* Progression to adrenocortical tumorigenesis in mice and humans through insulin-like growth factor 2 and β-catenin. *Am J Pathol* 2012; **181**: 1017–1033.
8 Drelon C, Berthon A, Ragazzon B, Tissier F, Bandiera R, Sahut-Barnola I *et al.* Analysis of the role of Igf2 in adrenal tumour development in transgenic mouse models. *PloS One* 2012; **7**: e44171.
9 Drelon C, Berthon A, Val P. Adrenocortical cancer and IGF2: is the game over or our experimental models limited? *J Clin Endocrinol Metab* 2013; **98**: 505–507.
10 Hisada M, Garber JE, Fung CY, Fraumeni JF, Li FP. Multiple primary cancers in families with Li-Fraumeni syndrome. *J Natl Cancer Inst* 1998; **90**: 606–611.
11 Ribeiro RC, Sandrini F, Figueiredo B, Zambetti GP, Michalkiewicz E, Lafferty AR *et al.* An inherited p53 mutation that contributes in a tissue-specific manner to pediatric adrenal cortical carcinoma. *Proc Natl Acad Sci USA* 2001; **98**: 9330–9335.
12 Latronico AC, Pinto EM, Domenice S, Fragoso MC, Martin RM, Zerbini MC *et al.* An inherited mutation outside the highly conserved DNA-binding domain of the p53 tumor suppressor protein in children and adults with sporadic adrenocortical tumors. *J Clin Endocrinol Metab* 2001; **86**: 4970–4973.
13 Libè R, Groussin L, Tissier F, Elie C, René-Corail F, Fratticci A *et al.* Somatic TP53 mutations are relatively rare among adrenocortical cancers with the frequent 17p13 loss of heterozygosity. *Clin Cancer Res* 2007; **13**: 844–850.
14 Reincke M, Karl M, Travis WH, Mastorakos G, Allolio B, Linehan HM *et al.* p53 mutations in human adrenocortical neoplasms: immunohistochemical and molecular studies. *J Clin Endocrinol Metab* 1994; **78**: 790–794.
15 Heinze B, Herrmann LJM, Fassnacht M, Ronchi CL, Willenberg HS, Quinkler M *et al.* Less common genotype variants of TP53 polymorphisms are associated with poor outcome in adult patients with adrenocortical carcinoma. *Eur J Endocrinol* 2014; **170**: 707–717.
16 Ragazzon B, Libé R, Assié G, Tissier F, Barreau O, Houdayer C *et al.* Mass-array screening of frequent mutations in cancers reveals RB1 alterations in aggressive adrenocortical carcinomas. *Eur J Endocrinol* 2014; **170**: 385–391.
17 de Reyniès A, Assié G, Rickman DS, Tissier F, Groussin L, René-Corail F *et al.* Gene expression profiling reveals a new classification of adrenocortical tumors and identifies molecular predictors of malignancy and survival. *J Clin Oncol* 2009; **27**: 1108–1115.
18 Giordano TJ, Kuick R, Else T, Gauger PG, Vinco M, Bauersfeld J *et al.* Molecular classification and prognostication of adrenocortical tumors by transcriptome profiling. *Clin Cancer Res* 2009; **15**: 668–676.
19 Assie G, Letouze E, Fassnacht M, Jouinot A, Luscap W, Barreau O *et al.* Integrated genomic characterization of adrenocortical carcinoma. *Nat Genet* 2014; **46**: 607–612.
20 Zheng S, Cherniack AD, Dewal N, Moffitt RA, Danilova L, Murray BA *et al.* Comprehensive pan-genomic characterization of adrenocortical carcinoma. *Cancer Cell* 2016; **29**: 723–736.
21 Kananen K, Markkula M, Mikola M, Rainio EM, McNeilly A, Huhtaniemi I. Gonadectomy permits adrenocortical tumorigenesis in mice transgenic for the mouse inhibin alpha-subunit promoter/simian virus 40 T-antigen fusion gene: evidence for negative autoregulation of the inhibin alpha-subunit gene. *Mol Endocrinol Baltim Md* 1996; **10**: 1667–1677.
22 Ragazzon B, Lefrançois-Martinez A-M, Val P, Sahut-Barnola I, Tournaire C, Chambon C *et al.* Adrenocorticotropin-dependent changes in SF-1/DAX-1 ratio influence steroidogenic genes expression in a novel model of glucocorticoid-producing adrenocortical cell lines derived from targeted tumorigenesis. *Endocrinology* 2006; **147**: 1805–1818.
23 Tissier F, Aubert S, Leteurtre E, Al Ghuzlan A, Patey M, Decaussin M *et al.* Adrenocortical tumors: improving the practice of the Weiss system through virtual microscopy: a National Program of the French Network INCa-COMETE. *Am J Surg Pathol* 2012; **36**: 1194–1201.

24 Lambert-Langlais S, Pointud J-C, Lefrançois-Martinez A-M, Volat F, Manin M, Coudoré F *et al.* Aldo keto reductase 1B7 and prostaglandin F2alpha are regulators of adrenal endocrine functions. *PloS One* 2009; **4**: e7309.
25 Hershkovitz L, Beuschlein F, Klammer S, Krup M, Weinstein Y. Adrenal 20alpha-hydroxysteroid dehydrogenase in the mouse catabolizes progesterone and 11-deoxycorticosterone and is restricted to the X-zone. *Endocrinology* 2007; **148**: 976–988.
26 Romero DG, Yanes LL, de Rodriguez AF, Plonczynski MW, Welsh BL, Reckelhoff JF *et al.* Disabled-2 is expressed in adrenal zona glomerulosa and is involved in aldosterone secretion. *Endocrinology* 2007; **148**: 2644–2652.
27 Tissier F, Louvel A, Grabar S, Hagnéré A-M, Bertherat J, Vacher-Lavenu M-C *et al.* Cyclin E correlates with malignancy and adverse prognosis in adrenocortical tumors. *Eur J Endocrinol* 2004; **150**: 809–817.
28 Beuschlein F, Weigel J, Saeger W, Kroiss M, Wild V, Daffara F *et al.* Major prognostic role of Ki67 in localized adrenocortical carcinoma after complete resection. *J Clin Endocrinol Metab* 2015; **100**: 841–849.
29 Drelon C, Berthon A, Mathieu M, Ragazzon B, Kuick R, Tabbal H *et al.* EZH2 is overexpressed in adrenocortical carcinoma and is associated with disease progression. *Hum Mol Genet* 2016; **25**: 2789–2800.
30 Libé R, Bertherat J. Molecular genetics of adrenocortical tumours, from familial to sporadic diseases. *Eur J Endocrinol* 2005; **153**: 477–487.
31 Gaujoux S, Grabar S, Fassnacht M, Ragazzon B, Launay P, Libé R *et al.* β-catenin activation is associated with specific clinical and pathologic characteristics and a poor outcome in adrenocortical carcinoma. *Clin Cancer Res* 2011; **17**: 328–336.
32 Ragazzon B, Libé R, Gaujoux S, Assié G, Fratticci A, Launay P *et al.* Transcriptome analysis reveals that p53 and {beta}-catenin alterations occur in a group of aggressive adrenocortical cancers. *Cancer Res* 2010; **70**: 8276–8281.
33 Berthon A, Sahut-Barnola I, Lambert-Langlais S, de Joussineau C, Damon-Soubeyrand C, Louiset E *et al.* Constitutive beta-catenin activation induces adrenal hyperplasia and promotes adrenal cancer development. *Hum Mol Genet* 2010; **19**: 1561–1576.
34 Bernichtein S, Petretto E, Jamieson S, Goel A, Aitman TJ, Mangion JM *et al.* Adrenal gland tumorigenesis after gonadectomy in mice is a complex genetic trait driven by epistatic loci. *Endocrinology* 2008; **149**: 651–661.
35 Surana R, Sikka S, Cai W, Shin EM, Warrier SR, Tan HJG *et al.* Secreted frizzled related proteins: Implications in cancers. *Biochim Biophys Acta* 2014; **1845**: 53–65.
36 Heikkila M, Peltoketo H, Leppaluoto J, Ilves M, Vuolteenaho O, Vainio S. Wnt-4 deficiency alters mouse adrenal cortex function, reducing aldosterone production. *Endocrinology* 2002; **143**: 4358–4365.
37 Gibb N, Lavery DL, Hoppler S. sfrp1 promotes cardiomyocyte differentiation in Xenopus via negative-feedback regulation of Wnt signalling. *Dev Camb Engl* 2013; **140**: 1537–1549.
38 Yamamura S, Kawakami K, Hirata H, Ueno K, Saini S, Majid S *et al.* Oncogenic functions of secreted Frizzled-related protein 2 in human renal cancer. *Mol Cancer Ther* 2010; **9**: 1680–1687.
39 Sun Y, Zhu D, Chen F, Qian M, Wei H, Chen W *et al.* SFRP2 augments WNT16B signaling to promote therapeutic resistance in the damaged tumor microenvironment. *Oncogene* 2016; **35**: 4321–4334.
40 Feng Z, Zhang H, Levine AJ, Jin S. The coordinate regulation of the p53 and mTOR pathways in cells. *Proc Natl Acad Sci USA* 2005; **102**: 8204–8209.
41 Paglin S, Yahalom J. Pathways that regulate autophagy and their role in mediating tumor response to treatment. *Autophagy* 2006; **2**: 291–293.
42 Doghman M, El Wakil A, Cardinaud B, Thomas E, Wang J, Zhao W *et al.* Regulation of insulin-like growth factor-mammalian target of rapamycin signaling by microRNA in childhood adrenocortical tumors. *Cancer Res* 2010; **70**: 4666–4675.
43 Doghman M, Lalli E. Efficacy of the novel dual PI3-kinase/mTOR inhibitor NVP-BEZ235 in a preclinical model of adrenocortical carcinoma. *Mol Cell Endocrinol* 2012; **364**: 101–104.
44 De Martino MC, van Koetsveld PM, Feelders RA, Sprij-Mooij D, Waaijers M, Lamberts SWJ *et al.* The role of mTOR inhibitors in the inhibition of growth and cortisol secretion in human adrenocortical carcinoma cells. *Endocr Relat Cancer* 2012; **19**: 351–364.
45 Papotti M, Libè R, Duregon E, Volante M, Bertherat J, Tissier F. The Weiss score and beyond--histopathology for adrenocortical carcinoma. *Horm Cancer* 2011; **2**: 333–340.
46 Berruti A, Fassnacht M, Haak H, Else T, Baudin E, Sperone P *et al.* Prognostic role of overt hypercortisolism in completely operated patients with adrenocortical cancer. *Eur Urol* 2014; **65**: 832–838.
47 Assié G, Guillaud-Bataille M, Ragazzon B, Bertagna X, Bertherat J, Clauser E. The pathophysiology, diagnosis and prognosis of adrenocortical tumors revisited by transcriptome analyses. *Trends Endocrinol Metab* 2010; **21**: 325–334.
48 Juhlin CC, Goh G, Healy JM, Fonseca AL, Scholl UI, Stenman A *et al.* Whole-exome sequencing characterizes the landscape of somatic mutations and copy number alterations in adrenocortical carcinoma. *J Clin Endocrinol Metab* 2015; **100**: E493–E502.
49 Baudin E. Endocrine Tumor Board of Gustave Roussy. Adrenocortical carcinoma. *Endocrinol Metab Clin North Am* 2015; **44**: 411–434.
50 Ahuja D, Sáenz-Robles MT, Pipas JM. SV40 large T antigen targets multiple cellular pathways to elicit cellular transformation. *Oncogene* 2005; **24**: 7729–7745.
51 Bocchetta M, Eliasz S, De Marco MA, Rudzinski J, Zhang L, Carbone M. The SV40 large T antigen-p53 complexes bind and activate the insulin-like growth factor-I promoter stimulating cell growth. *Cancer Res* 2008; **68**: 1022–1029.
52 Fassnacht M, Terzolo M, Allolio B, Baudin E, Haak H, Berruti A *et al.* Combination chemotherapy in advanced adrenocortical carcinoma. *N Engl J Med* 2012; **366**: 2189–2197.
53 Fassnacht M, Berruti A, Baudin E, Demeure MJ, Gilbert J, Haak H *et al.* Linsitinib (OSI-906) versus placebo for patients with locally advanced or metastatic adrenocortical carcinoma: a double-blind, randomised, phase 3 study. *Lancet Oncol* 2015; **16**: 426–435.
54 Feng Z, Levine AJ. The regulation of energy metabolism and the IGF-1/mTOR pathways by the p53 protein. *Trends Cell Biol* 2010; **20**: 427–434.
55 Martino MCD, Feelders RA, de Herder WW, van Koetsveld PM, Dogan F, Janssen JAMJL *et al.* Characterization of the mTOR pathway in human normal adrenal and adrenocortical tumors. *Endocr Relat Cancer* 2014; **21**: 601–613.
56 Naing A, Kurzrock R, Burger A, Gupta S, Lei X, Busaidy N *et al.* Phase I trial of cixutumumab combined with temsirolimus in patients with advanced cancer. *Clin Cancer Res* 2011; **17**: 6052–6060.
57 Gangadhar TC, Cohen EEW, Wu K, Janisch L, Geary D, Kocherginsky M *et al.* Two drug interaction studies of sirolimus in combination with sorafenib or sunitinib in patients with advanced malignancies. *Clin Cancer Res* 2011; **17**: 1956–1963.
58 Fraenkel M, Gueorguiev M, Barak D, Salmon A, Grossman AB, Gross DJ. Everolimus therapy for progressive adrenocortical cancer. *Endocrine* 2013; **44**: 187–192.

Supplementary Information accompanies this paper on the Oncogene website (http://www.nature.com/onc)